



Temporal patterns and drivers of CO₂ emission from dry sediments in a groyne field of a large river

Matthias Koschorreck¹, Klaus Holger Knorr², and Lelaina Teichert^{1,2}

¹Department of Lake Research, Helmholtz Centre for Environmental Research – UFZ, Magdeburg, 39114, Germany

²Institute of Landscape Ecology, University of Münster Münster, Germany

Correspondence: Matthias Koschorreck (matthias.koschorreck@ufz.de)

Received: 4 March 2022 – Discussion started: 11 March 2022

Revised: 30 September 2022 – Accepted: 12 October 2022 – Published: 18 November 2022

Abstract. River sediments falling dry at low water levels are sources of CO₂ to the atmosphere. While the general relevance of CO₂ emissions from dry sediments has been acknowledged and some regulatory mechanisms have been identified, knowledge on mechanisms and temporal dynamics is still sparse. Using a combination of high-frequency measurements and two field campaigns we thus aimed to identify processes responsible for CO₂ emissions and to assess temporal dynamics of CO₂ emissions from dry sediments at a large German river.

CO₂ emissions were largely driven by microbial respiration in the sediment. Observed CO₂ fluxes could be explained by patterns and responses of sediment respiration rates measured in laboratory incubations. We exclude groundwater as a significant source of CO₂ because the CO₂ concentration in the groundwater was too low to explain CO₂ fluxes. Furthermore, CO₂ fluxes were not related to radon fluxes, which we used to trace groundwater-derived degassing of CO₂.

CO₂ emissions were strongly regulated by temperature resulting in large diurnal fluctuations of CO₂ emissions with emissions peaking during the day. The diurnal temperature–CO₂ flux relation exhibited a hysteresis which highlights the effect of transport processes in the sediment and makes it difficult to identify temperature dependence from simple linear regressions. The temperature response of CO₂ flux and sediment respiration rates in laboratory incubations was identical. Also deeper sediment layers apparently contributed to CO₂ emissions because the CO₂ flux was correlated with the thickness of the unsaturated zone, resulting in CO₂ fluxes increasing with distance to the local groundwater level and with distance to the river. Rain events lowered CO₂ emissions from dry river sediments probably by blocking CO₂

transport from deeper sediment layers to the atmosphere. Terrestrial vegetation growing on exposed sediments greatly increased respiratory sediment CO₂ emissions. We conclude that the regulation of CO₂ emissions from dry river sediments is complex. Diurnal measurements are mandatory and even CO₂ uptake in the dark by phototrophic microorganisms has to be considered when assessing the impact of dry sediments on CO₂ emissions from rivers.

1 Introduction

1.1 CO₂ emissions from dry river sediments – significance

Streams and rivers are known to play an important role in the global carbon cycle. The transport of continental carbon to the ocean is mainly regulated by rivers (Schlesinger and Melack, 1981). Moreover, carbon in rivers undergoes transformation processes and can be temporarily stored by means of sedimentation and photosynthesis or released due to biological respiration (Battin et al., 2009). One distinctive feature of rivers is their frequently changing water level. Climate change is expected to further increase the seasonal and the inter-annual variability of rivers and hydrological regimes (Bolpagni et al., 2019; Coppola et al., 2014). In Europe, more frequent and longer-lasting droughts are expected during summers, which lead to low water levels in streams and rivers (Spinoni et al., 2018). Consequently, previously submerged river sediment will be exposed to the atmosphere and influenced by drying (Steward et al., 2012). It has been shown that these exposed sediments can emit high amounts

of CO₂ (von Schiller et al., 2014) and may represent a globally relevant carbon source to the atmosphere (Marcé et al., 2019).

1.2 Regulation of CO₂ emissions from dry sediments

While the relevance of CO₂ emissions from dry river sediments has been acknowledged, only little is known about underlying mechanisms and temporal patterns. A recent study identified organic matter content and moisture as common drivers of CO₂ emissions from dry aquatic sediments (Keller et al., 2020). However, high variability prevents the prediction of CO₂ fluxes for particular sites. Case studies showed that CO₂ emissions are affected by temperature (Doering et al., 2011), emergent vegetation (Bolpagni et al., 2017), organic matter (Palmia et al., 2021), water content (Martinsen et al., 2019), or the frequency of dry–wet cycles (Machado dos Santos Pinto et al., 2020). Although it is known that CO₂ emission from dry sediment may change with time, existing studies are based on single or few measurements. Few studies addressed temporal variability of CO₂ emissions, but nothing is yet known about short-term dynamics of greenhouse gas (GHG) emissions from dry aquatic sediments. Investigating temporal variability of CO₂ fluxes should provide information about the potential sources of emitted CO₂. Knowing sources of emitted CO₂ from dry sediments is crucial to be able to model or scale up GHG emissions from these systems.

1.3 Possible sources of CO₂

Carbon emissions from desiccated sediments derive from a number of possible biotic and abiotic sources (Marcé et al., 2019). Microbial respiration is known to contribute to CO₂ emissions (Weise et al., 2016), similar to soil respiration. Organic matter originating from organic particle sedimentation may be mineralized to CO₂ or CH₄. It is typically observed that CH₄ emissions from dry sediments are low, indicating that anaerobic mineralization plays a minor role (Marcé et al., 2019).

In contrast to respiration, abiotic processes are rarely taken into account as sources of CO₂ (Rey, 2015). Yet, recent findings revealed a spatial variability of CO₂ fluxes from dry river sediments with highest fluxes near to the river (Mallast et al., 2020). As a possible explanation, the authors hypothesized that at decreasing river water level a groundwater flow gradient towards the river would transport groundwater to the river (Peters et al., 2006). Groundwater is usually 10- to 100-fold super-saturated with CO₂ (Macpherson, 2009). Near to the river the thickness of the unsaturated layer approaches zero and CO₂ rich groundwater reaches the surface sediment where CO₂ would eventually degas.

1.4 Aim of study

Given the uncertainty of the origin of CO₂ emitted from dry river sediments, in this study we aimed to test the hypothesis of Mallast et al. (2020) that CO₂ emissions from dry sediments of larger rivers are driven by groundwater degassing. If groundwater was a significant source of CO₂, we hypothesize a only weak temperature dependence of CO₂ emissions. We applied a combination of automatic high-frequency measurements and detailed studies using a variety of methods to identify the source of CO₂ emissions from dry sediments at a large German river and to understand their temporal dynamics and drivers.

2 Material and methods

2.1 Study site

The study was conducted at the lowland part of the river Elbe, one of the largest rivers in central Europe with a discharge average of about 559 m³ s⁻¹ at the city of Magdeburg (Weigold and Baborowski, 2009). Near Magdeburg, the middle Elbe can be characterized as a free-flowing, lowland river with comparable large floodplains, only regulated by groyne fields. Such groyne fields are the dominant shore type along the German part of the river (Bussmann et al., 2022).

Hence, seasonal water level fluctuations are shaping the different habitats alongside the river, ranging from alluvial forests and pastures to sandy beaches (Scholten et al., 2005). The study site is located near the farm “Apfelwerder” at river km 314 in between two groins and is characterized by a slight slope from the river to the adjoining pasture (52.038398° N, 11.715495° E). Groynes extended about 50 m into the river, and distance between groynes was 130±37 m. A sandy beach of about 2 to 5 m with sparse vegetation (*Persicaria lapathifolia*, *Rorippa amphibia*, *Polygonum aviculare*) could be found directly at the river, while the vegetation became denser with distance to the river (Fig. S1 in the Supplement).

2.2 High-frequency measurements

2.2.1 Automatic flux chambers, water table levels, and environmental data

To cover the temporal dynamics of CO₂ fluxes three opaque automatic chambers (CFLUX-1 Automated Soil CO₂ Flux System, PP systems, Amesbury, Massachusetts, USA), were installed (Fig. S1). The chambers measured CO₂ fluxes once every hour. Each flux measurement lasted 5 min and between flux measurements the chambers were open for 55 min. CO₂ fluxes were calculated from the linear increase of CO₂ during a closure time of 5 min. Each chamber was equipped with a soil moisture and temperature probe (Stevens HydraProbe, Stevens Water Monitoring Systems, Portland, Oregon, USA). Due to fluctuating water levels over the summer of 2020

(Fig. 1), it was not possible to measure CO₂ fluxes from the sediment continuously over the whole measurement period. The chambers were set up in the periods from 1 May to 10 June, from 3 to 6 August, and from 17 to 26 September; moreover, during deployment they needed to be moved occasionally. Automatic flux chamber data were discarded when the collar was flooded or the sand was washed away by waves, which resulted in CO₂ concentrations fluctuating around ambient concentration. The final dataset contained 3128 flux measurements.

Because we did not know the exact elevation of our research site, we installed the chambers at defined heights relative to the gauge “Magdeburg Strombrücke” (located 13 km downstream of the study side, zero point of gauge = 39.885 m above mean sea level; ELWIS, 2020). Therefore, the distance to the river and the height over water level were determined once, along a transect. Out of these parameters, a slope was calculated and afterward used to position the automatic chambers in the field. Positions, where the automatic chambers were placed were related to gauge levels 75, 85, and 95 cm. In other words: when the gauge recorded a water level of, e.g., 75, a chamber at the “75 cm position” was located directly above the water line at our research site. The thickness of the unsaturated sediment was calculated as the difference between the height above zero gauge for each chamber and the actual river level. Weather data from the German Weather Service were obtained for the monitoring station Magdeburg 15 km from Apfelwerder (DWD, 2020).

2.2.2 High-resolution sediment respiration flux transects

To investigate spatial variability, between May and September, transects of sediment respiration were measured with a portable soil respiration system (EGM-5 Portable CO₂ Gas Analyzer + soil respiration chamber, PP Systems, Amesbury, Massachusetts, USA) equipped with the same soil moisture and temperature probe as the automatic chambers. On each occasion 12 flux measurements along a 15 m long transect from the water upslope were recorded. The opaque chamber was placed on vegetation-free spots to make sure that sediment respiration was measured. At each measuring spot we took note whether plants were growing nearby.

2.3 Detailed sampling campaigns

To more closely investigate the mechanisms behind the CO₂ flux, two intensive measurement campaigns were carried out on 4 August 2020 and 23 September 2020.

2.3.1 Manual chamber measurements

To quantify CO₂ fluxes at different distances to the river and also check for CH₄ emissions, manual chamber measurements were done in 1 m steps away from the flowing water, along a transect which was characterized by an uphill slope

of ~ 11.5 %. Collars (39 cm diameter) were installed at four sites along the transect a day in advance to minimize disturbance during measurements (Fig. S1b). For flux measurements, an opaque chamber ($V = 0.0239 \text{ m}^3$, $A = 0.1195 \text{ m}^2$) equipped with a pressure vent tube was placed on a collar. The concentrations in the chamber were measured every 30 s for ~ 5 min with a multicomponent Fourier-transform infrared (FTIR) gas analyzer (DX4000, Gaset Technologies GmbH, Helsinki, Finland). The FTIR gas analyzer continuously measures CO₂, CH₄, and nitrous oxide (N₂O) with an accuracy of $\pm 4 \text{ ppm CO}_2$ and $\pm 0.1 \text{ ppm CH}_4$ and N₂O (Gaset Technologies GmbH 2018). Hence, the detection limit of the CO₂ flux was $\sim 2 \text{ mmol m}^{-2} \text{ d}^{-1}$, while the CH₄ flux was detectable if above $0.12 \text{ mmol m}^{-2} \text{ d}^{-1}$ and for N₂O if above $0.2 \text{ mmol m}^{-2} \text{ d}^{-1}$. Fluxes were calculated from the linear increase of the respective gas mixing ratio (Gómez-Gener et al., 2015) with time using the R package glimr (Keller, 2020).

2.3.2 Rn sediment efflux measurements

To assess groundwater degassing, ²²²Rn measurements were performed. The geogenic gas ²²²Rn is a commonly used natural tracer for groundwater influence in aquatic systems and is additionally known as a useful tool to trace the origins of CO₂ (Cook and Herczeg, 2000). Therefore, ²²²Rn concentrations and fluxes were measured with a portable radon detector (RAD7 Radon Detector, DURRIDGE, Billerica, Massachusetts, USA) to determine the groundwater influence on CO₂ fluxes from dry river sediments. The measurements of the RAD7 are based on electrostatic collection of alpha emitters with spectral analysis. Measuring with the “Normal” mode counts decays of both polonium decay products of ²²²Rn (²¹⁸Po, ²¹⁴Po). The counts were measured over 1 h and averaged, with a 1 σ standard deviation and expresses as decays per second [Bq]. The measurement range lies between 4–750 000 Bq m⁻³ with an accuracy of $\pm 5 \%$.

The ²²²Rn concentration in 300 mL samples from groundwater (2.3.3) and the river was measured with the Wat250 mode. In addition, soil ²²²Rn emissions were estimated with closed chamber measurements with the RAD7 over 3 h (one Rn measurement per hour). Assuming that groundwater is the main source of CO₂ and that ²²²Rn moves at the same mass flow as CO₂ (Megonigal et al., 2020), the same spatial dependence of CO₂ and ²²²Rn fluxes would be expected in the case of groundwater being the major source of CO₂. For this reason, ²²²Rn chamber measurements were performed simultaneously at two different positions: one with low and one with high CO₂ flux. We used two chambers of different sizes and corrected ²²²Rn flux measurements [$\text{Bq m}^{-3} \text{ d}^{-1}$] for different chamber geometry by multiplying with the volume [m^3] and dividing by the area [m^2] of the chamber to get the ²²²Rn flux [$\text{Bq m}^{-2} \text{ d}^{-1}$].

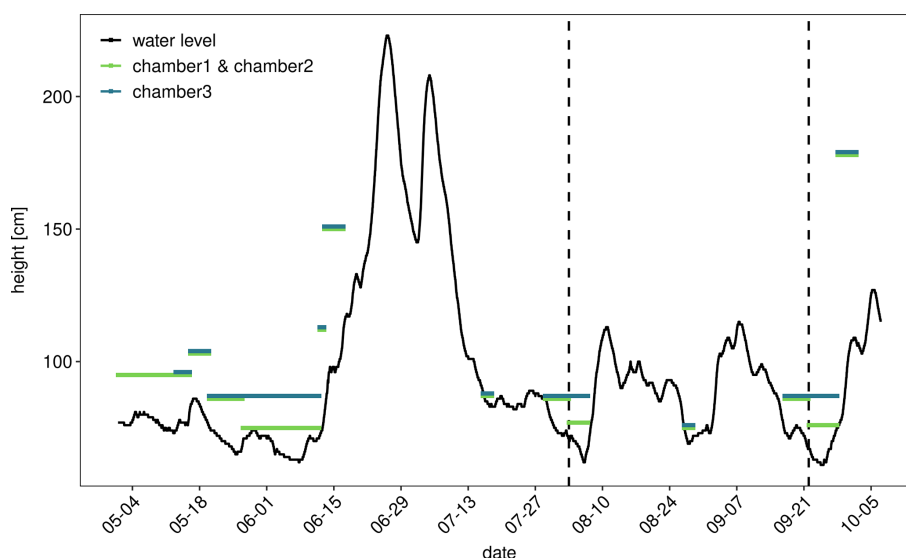


Figure 1. Water level of the Elbe River at gauge Magdeburg Strombrücke (13 km downstream) in summer 2020. Colored lines indicate positioning of automatic flux chambers. For example a horizontal line at 95 cm means that a particular chamber was located at the water line when the gauge recorded a water level of 95 cm. Vertical dotted lines indicate intensive sampling campaigns.

2.3.3 Water + sediment sampling

For groundwater, sampling piezometers with a diameter of 2.7 cm and a length of 100 cm were installed next to each collar (Fig. S1b) a day before the sampling campaign.

To determine the thickness of the unsaturated zone, the water level in the piezometers was measured with an electric contact gauge. In situ parameters pH, conductivity, temperature, and O₂ saturation were measured in the piezometers and the river with a multiparameter probe (WTW® MultiLine® Multi 3630 IDS, Xylem, Rye Brook, New York, USA). To analyze dissolved CO₂ and CH₄ concentrations, water samples were taken from the piezometers and the river using a syringe. Atmospheric air was added, with a headspace ratio of 1 : 1. After shaking for 2 min the headspace was transferred to 12 mL evacuated Exetainers (Labco Exetainers®, Labco Limited, Lampeter, UK) and stored till further analysis in the laboratory. Air samples were taken for headspace correction. Water samples for chemical analysis were collected in crimp vials without a headspace, stored at 4 °C, and later analyzed in the laboratory.

Soil samples from the 0–5 cm layer were taken around each collar for incubation experiments. Samples were filled into plastic bags, were stored at 4 °C, and analyzed in the laboratory within a week.

2.3.4 Potential CO₂ production in laboratory incubations of sediment

Incubation experiments were set up to analyze the potential microbial respiration in dry river sediments under controlled conditions. For this purpose, fresh soil samples (25 g wet

weight) taken along the transect were incubated in ~ 130 mL vials in replicates of four at 19.5 °C. To determine the temperature dependence of microbial respiration, four replicate samples of 25 g were incubated at 4, 12, 19.5, 28, and 35 °C. From each vial, four to five gas samples were taken over an incubation period of 2 to 3 d by a Pressure-Lok® syringe (Pressure-Lok® glass syringe, Valco Instruments, Houston, Texas, USA) and analyzed by gas chromatography for CO₂. Respiration rates were calculated from the linear increase of the CO₂ content in the incubation vials divided by dry sediment weight.

To evaluate the temperature response of the microbial respiration in the sediment the Q_{10} temperature coefficient and the activation energy (E_a) was calculated (Dell et al., 2011). The activation energy was calculated as the slope of Arrhenius plots as described in Gillooly et al. (2001).

To compare respiration data from lab incubations to CO₂ fluxes measured in the field rates, rates of respiration per gram dry weight [$\mu\text{mol g-dw d}^{-1}$] were converted to fluxes by multiplying with sediment bulk density [g-dw cm^{-3}] and the thickness of the reactive sediment layer which we assume to be equal to the thickness of the unsaturated zone [cm].

2.4 Analytics

CO₂ and CH₄ concentrations in gas samples were measured with a gas chromatograph (GC) (SRI 8610C, SRI Instruments Europe, Bad Honnef, Germany). The GC was equipped with a flame ionization detector and a methanizer which allowed for simultaneous measurement of CO₂ and CH₄ with an accuracy of < 5 %. Dissolved gas concentrations were calculated using temperature-dependent Henry

coefficients (UNESCO/IHA, 2010). Because the carbonate system in the headspace vial may change during headspace equilibration, CO₂ concentrations were corrected for alkalinity as described in Koschorreck et al. (2021).

To analyze dissolved inorganic carbon (DIC), and dissolved organic carbon (DOC) water samples were filtered with a glass microfiber filter (Whatman GF/F). DIC and DOC concentrations were analyzed based on high-temperature oxidation and nondispersive infrared (NDIR) detection (DIMATOC[®] 2000, DIMATEC Analysentechnik, Essen, Germany). The alkalinity of the water samples was determined by titration with HCl to pH of 4.3. To determine the concentration of the cations K⁺, Na⁺, Ca²⁺, and Mg²⁺, the water samples were filtered with a 0.45 µm syringe filter, acidified with HNO₃, and analyzed with an inductively coupled plasma optical emission spectrometer (ICP OES) (Optima 7300 DV, PerkinElmer, USA). The anion concentrations of SO₄²⁻ and Cl⁻ were measured with ion chromatography (Dionex ICS 6000, Thermo Fisher Scientific, Waltham, Massachusetts, USA).

Soil samples were analyzed to determine soil moisture content, bulk density, and organic matter from weight loss after drying for at least 2 d to constant weight at 105 °C and loss on ignition (LOI) at 550 °C, respectively. Sediment texture was determined by the FAO method (FAO, 2020).

2.5 Statistics

CO₂ flux datasets from manual and automatic measurements were visually checked for normal distribution with Q–Q plots. Data were summarized by distance to the river and tested with a one-sample *t* test to determine if measured fluxes differed significantly from zero.

Spearman rank correlation was used to identify relationships between environmental variables and the observed CO₂ flux and to identify the strength and direction of these relations (Leyer and Wesche, 2007). Additionally, representative periods and single days were selected from automatic measurements to analyze patterns hidden by the temporal variability of the data. The measured environmental variables of sediment temperature, sediment moisture, thickness of the unsaturated zone, organic matter content, and precipitation were used for correlation analysis. Water level and climate data were averaged over 1 h. Linear mixed-effects models (LMEs) were applied to predict the influence of the environmental variables on the CO₂ flux at the study site for variables for which a linear relationship with the CO₂ flux was presumed. Model selection was done by removing predictors and comparing conditional *R*² values of different models. To apply simple linear regression models and LMEs, assumptions of normality and homoscedasticity were visually checked with diagnostic plots, including residuals vs. fitted and Q–Q plot. Flux data were log-transformed for LME analysis. Because of occasional small negative fluxes, we shifted all fluxes to positive values by adding 121 mmol m⁻² d⁻¹

prior to transformation (120 was the value of the largest negative flux). Statistical analysis was performed using R (R-Core-Team, 2016).

3 Results

3.1 Long-term data

The river showed a typical summer discharge situation with a water level mostly below 1 m, interrupted by a high-discharge event at the end of June (Fig. 1). Considerable areas of dry sediments only emerged during 6 weeks in early summer and short periods in the first week of August and in September. CO₂ fluxes measured during these periods showed high diurnal and seasonal fluctuations (Fig. 2). Fluxes fluctuated over 3 orders of magnitude between –120 and 1135 mmol m⁻² d⁻¹ with a median of 98 and a mean ± SD of 149 ± 155 mmol m⁻² d⁻¹. Fluxes fluctuated in a narrow range below 200 mmol m⁻² d⁻¹ during the first phase of the investigations in May. Due to rising water level, on 17 May we moved the chambers higher up where we measured both higher fluxes and larger diurnal amplitudes. When the water level decreased after 20 May, we moved the chamber down to freshly emerged sediment. There, CO₂ fluxes were similar to the fluxes measured 10 cm higher during the first half of May and tended to increase with increasing time since drying. Negative fluxes were observed in 193 out of 3128 flux measurements (= 6 % of all fluxes). Negative fluxes were observed especially during the beginning of the measurement period and at sites near to the water. Interestingly, negative fluxes nearly exclusively occurred during the day between 10:00 and 18:00, peaking in the afternoon (Fig. S2). Chambers installed closer to the water measured lower and less variable fluxes than chambers installed higher up slope.

Fluxes showed considerable short-term variability. Variability was not constant during the investigated period but especially high after June. Clear diurnal patterns were observed during the entire study but most pronounced in September.

3.1.1 Regulatory factors: sediment moisture, temperature, water level, climate

The observed diurnal pattern with higher CO₂ fluxes during the day suggested a temperature regulation of the flux. The CO₂ flux was indeed weakly (Spearman *p* < 0.05) correlated with the thickness of the unsaturated zone (*R*² = 0.31), sediment temperature (*R*² = 0.19, Fig. 3a), and moisture (*R*² = –0.19), as well as precipitation (*R*² = –0.12). A linear mixed-effects model with site where the chamber was placed as random factor and temperature and thickness of the unsaturated zone as fixed factors explained 0.61 % of the variability. Adding moisture did not further improve the LME (Table S1 in the Supplement).

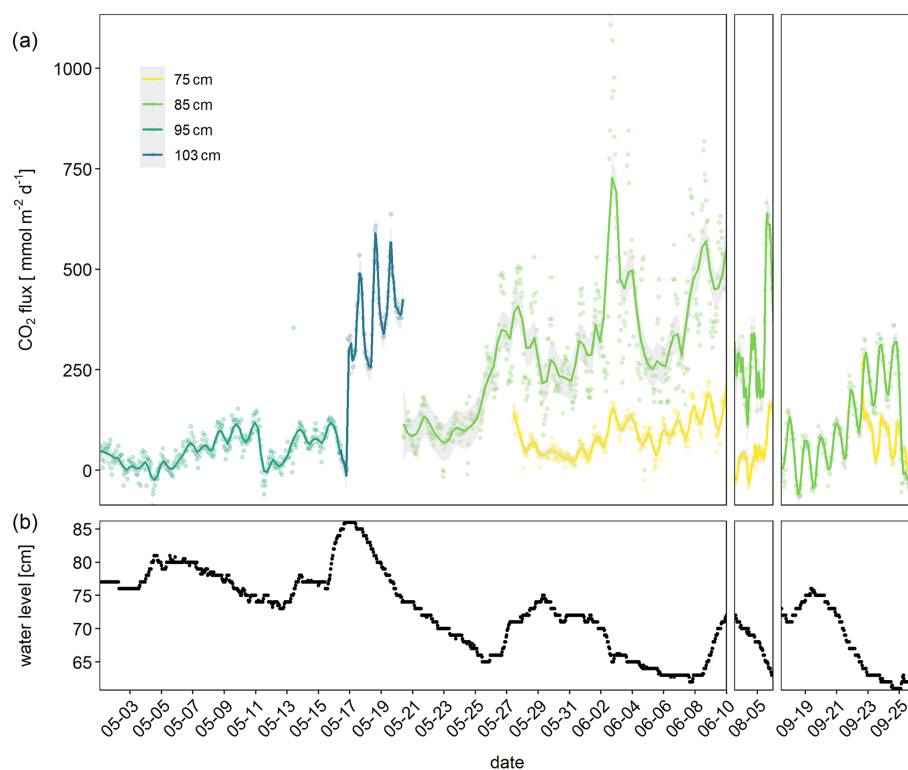


Figure 2. CO₂ fluxes in millimole per square meter per day measured with automatic chambers (a) and corresponding water level of the river measured 13 km downstream at the gauge Magdeburg Strombrücke (b). Colors indicate the elevation of the chambers. For example the 75 cm position means that the chamber was directly above the water line when the gauge reading was 75. Lines indicate smoothed data \pm SD using locally estimated scatterplot smoothing (LOESS) smoother with a span 0.1. The grey areas indicate confidence intervals.

The temperature response of the CO₂ flux was not very clear, however, if all data were plotted together (Fig. 3a), but if data from single days were plotted, a clear pattern emerged (Figs. 3b and S3). The temperature response of the flux was affected by the time of day resulting in typical hysteresis curves. Warming during the day resulted in exponentially increasing fluxes. However, fluxes stayed high despite cooling which started in the afternoon – the temperature response of the flux was clearly delayed. From the CO₂ flux–temperature relation (Fig. 3a) an activation energy of 0.56 eV (37 kJ mol^{−1}) could be calculated which corresponds to a Q_{10} of 1.7 between 10 and 20 °C.

A closer look at data from a single week in September revealed how temperature, thickness of the unsaturated zone, and precipitation interacted in regulating the flux (Fig. 4). Temperature drove the very clear diurnal amplitude, but the absolute level of the flux was higher with increasing thickness of the unsaturated zone (which was accompanied by sediment drying). A single precipitation event on 25 September resulted in a sudden increase in sediment moisture which was accompanied by a clear drop of the CO₂ flux. If only data for the period shown in Fig. 4 were considered, a linear model containing sediment temperature and moisture and

the interaction between temperature and moisture explained 46 % of the variance.

3.1.2 Spatial gradient of CO₂ flux

Manual chamber measurements at different distances to the water revealed a spatial gradient of the CO₂ flux. CO₂ fluxes were lowest near to the water line where sediment moisture was highest (Fig. 5) and fluxes increased with distance to the water. This was also visible in the automatic chamber data when chambers were placed at different distances to the water (compare Fig. 2). The chamber which was placed nearer to the water recorded consistently lower fluxes. This is also consistent with the observed positive correlation between CO₂ flux and the thickness of the unsaturated zone.

We also observed higher CO₂ fluxes in the vicinity of plants. Plants were consistently found from about 3 m from the water uphill. Fluxes above this “plant line” (indicated by the white line in Fig. 5) tended to be higher than fluxes from the vegetation-free area nearer to the water.

In sum, our field-based measurements provide strong evidence that respiration in the sediment was the major driver of the observed CO₂ flux. To further support this conclusion detailed investigations were carried out.

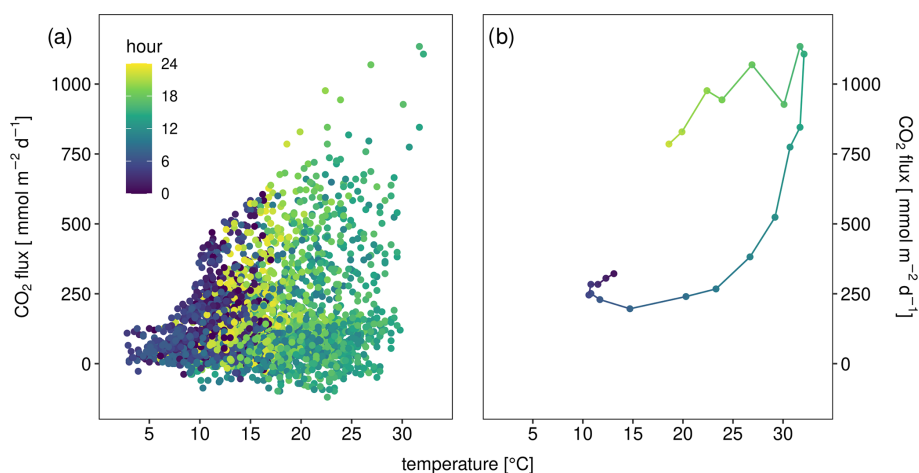


Figure 3. CO₂ flux in millimole per square meter per day (obtained from three automatic chambers) depending on sediment temperature of (a) all data and (b) only data from 2 June as an example for hysteretic response to temperature. Color indicates hour of measurement.

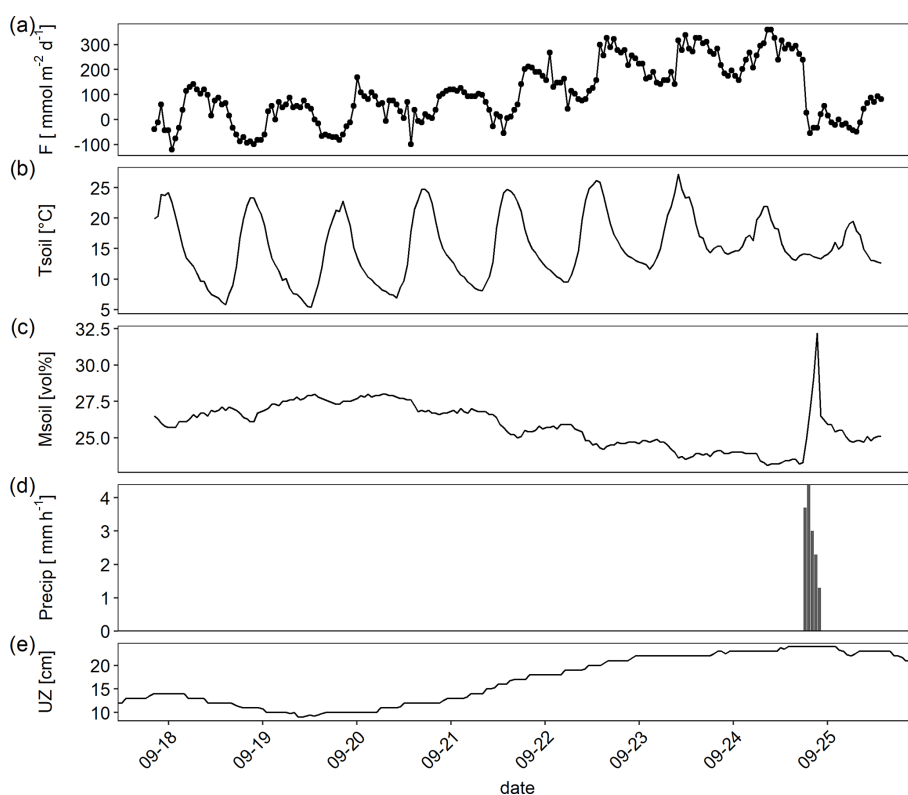


Figure 4. Example high-frequency dataset showing (a) CO₂ flux (F) measured by an automatic chambers, (b) sediment temperature (T_{soil} ; 0–5 cm depth), (c) sediment moisture (M_{soil} ; 0–5 cm depth) (d) precipitation (Precip) recorded in hourly resolution, and (e) thickness of the unsaturated zone (UZ; distance between water table level and ground surface).

3.2 Detailed investigations

The sediment pore water was quite similar to river water with respect to electric conductivity and dissolved solutes including DIC (Table 1). The water level difference between the wells and the river was below the detection limit – the hy-

draulic gradient was virtually zero during our sampling campaigns. The shallow hydraulic gradient and the similar chemistry suggest a large influence of river water on the sediment pore water. In contrast, concentrations of dissolved gases were quite different with high concentrations of CO₂ and CH₄ and low concentrations of O₂ in the pore water. Pore

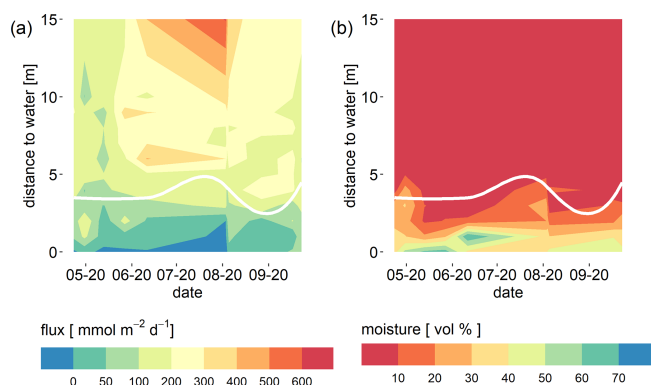


Figure 5. CO₂ flux ($\text{mmol m}^{-2} \text{d}^{-1}$) as measured with a manual chamber (a) and sediment moisture (vol %) measured with a probe in 0–5 cm depth (b) depending on the distance to the water. The white lines indicates the plant line. The area below this line was free of vegetation. There were never plants inside chambers.

water concentrations of CO₂ increased with distance to the river, while CH₄ concentrations tended to be highest near to the river. In August, the river water was slightly undersaturated with respect to CO₂. The sediment was poor in organic matter (LOI < 1 %) and texture was loamy sand. GHG emissions were dominated by CO₂, while CH₄ fluxes were low and N₂O fluxes were always below the detection limit (Table 1).

3.2.1 CO₂ fluxes versus Rn fluxes

Groundwater contained more than 1 order of magnitude higher Rn concentrations than the river water (Table 2). As an indicator of groundwater degassing and possible evasion of CO₂, we measured the flux of radon out of the sediment, assuming groundwater as a major source. Rn fluxes were higher in September than in August although the Rn concentration in the groundwater was similar in both months (Table 2). The flux of radon out of the sediment was, however, not much different at two different distances to the river, while the CO₂ flux differed by about 1 order of magnitude between the same sites. If groundwater was the source of CO₂, we would expect Rn fluxes to be related to CO₂ evasion from groundwater; thus our data indicate that higher CO₂ fluxes were not originating from groundwater.

3.2.2 Sediment respiration rates

To check whether the observed CO₂ fluxes could be explained by microbial respiration in the sediment, laboratory incubations were carried out. Sediment respiration rates as measured in laboratory incubations were $0.9 \pm 0.45 \mu\text{mol g}^{-1} \text{d}^{-1}$ in August and $0.64 \mu\text{mol g}^{-1} \text{d}^{-1}$ in September with rates increasing with distance to the river. Potential CO₂ fluxes calculated from these rates were similar or higher than CO₂ fluxes measured in situ (Fig. 6).

Thus, sediment respiration was high enough to explain the observed CO₂ emissions.

3.2.3 Temperature dependence of sediment respiration

Sediment respiration increased exponentially with temperature (Fig. 7) resulting in a Q_{10} of 2.5. The calculated activation energy of 0.7 eV was similar to the activation energy calculated from the automatic chamber data. The comparison with the temperature response of the CO₂ flux measured by the automatic chambers (line in Fig. 7) visualizes the similar temperature response of sediment respiration and in situ fluxes.

4 Discussion

4.1 Source of the CO₂

Both our continuous data and detailed measurements show that the CO₂ emitted from dry Elbe sediments originated from respiration in the sediment rather than from groundwater. This conclusion is consistently supported by numerous pieces of evidence:

- The observed CO₂ fluxes could be fully explained by sediment respiration measured in laboratory incubations. From soil respiration measurements, it is known that basal respiration as measured in laboratory incubations cannot be equivalent to soil CO₂ emissions (Reichstein et al., 2000). A major difference between both methods is the exclusion of root respiration in bottle incubations which would lead to an underestimation of total soil respiration in root-free assays such as bottle incubations (Hanson et al., 2000). Thus, our sediment respiration rates measured in the laboratory are probably conservative estimates which even strengthens our argumentation.
- The temperature response of the CO₂ flux was very similar to the measured temperature response of sediment respiration and showed Q_{10} values typical for biological processes (Yvon-Durocher et al., 2012) and soil respiration (Hamdi et al., 2013). Potential evaporation on the other hand depends on radiation, vapor pressure, and wind speed (Penman, 1948) and only indirectly on surface temperature (Kidron and Kronenfeld, 2016). The temperature dependence of evaporation of soils depends on a complex interaction of texture and soil moisture and is not easy to predict (e.g., Federer, 2002). The observed temperature dependence provides strong evidence for respiration being the primary driver of the CO₂ flux.
- CO₂ emissions increased with distance to the river. If groundwater was a major source of CO₂ emissions, we

Table 1. Sediment, groundwater, and river water properties at the two sampling campaigns.

Parameter	Unit	4 August 2020					23 September 2020				
Distance to river	m	river	1	3	5	6	river	1	2	3	4
CO ₂ flux	mmol m ⁻² d ⁻¹	–3	33	87	153	153	36	103	49	142	126
CH ₄ flux	mmol m ⁻² d ⁻¹	0.7	3.4	0	0	0.6	6	0.5	0	0	–0.6
Unsaturated zone	cm	–	10	31	62	78	–	9	19	32	36.5
Moisture	[vol %]	–	30	13	25	12	–	30	25	–	9
Organic matter in sediment	[% LOI]	–	0.78	0.39	1.11	0.94	–	0.85	0.97	–	0.52
CH ₄	μmol L ⁻¹	0.3	18	11	11	6	2.5	189	186	212	70
CO ₂	μmol L ⁻¹	13.3	610	883	1960	3681	32	1193	899	1118	1024
DIC	mg L ⁻¹	42	23	48	49	50	24	70	64	64	55
Alkalinity	mg L ⁻¹	1.9	3.5	3.5	3.6	3.1	1.9	4.5	4.8	5.3	4.7
DOC	mg L ⁻¹	13.1	6.9	9.3	12	13.5	6.31	9.4	9.9	11.5	11
SO ₄ ^{2–}	mg L ⁻¹	79	44	71	67	74	79	7.3	20	31	92
pH		8.3	7.2	6.8	6.6	6.6	8	7.2	7.3	7.2	7
Conductivity	μS cm ⁻¹	640	610	658	640	1563	601	696	655	647	640
O ₂	mg L ⁻¹	9.1	0.8	1.1	1.9	2	9.3	3.4	2.5	4	4

Diffusive fluxes from the river were calculated from concentrations using the gas transfer coefficient from Matoušů et al. (2019).

Table 2. Flux of radon measured as ²²²Rn increase in static chambers compared to CO₂ flux measured in the same chambers and radon concentration determined as detected activity [Bq m⁻³] in the groundwater sampled in wells directly beside the chambers as well as in the river water (0 m distance).

Date	Distance to river [m]	²²² Rn flux [Bq m ⁻² d ⁻¹]	CO ₂ flux [mmol m ⁻² d ⁻¹]	²²² Rn in water [Bq m ⁻³]
5 August	0			327 ± 109
	1	65	18 ± 20	6090 ± 418
	3	63	110 ± 31	
23 September	0			532 ± 135
	1	174	7 ± 41	6650 ± 436
	4	205	169 ± 36	

would expect higher emissions at lower sediment elevation where groundwater potentially exfiltrated into the sediment. If there was a hydraulic groundwater gradient towards the river, this gradient should be steepest near to the river resulting in highest groundwater flux and potential outgassing near the river.

- The CO₂ flux was proportional to the volume of the unsaturated sediment. If CO₂ originated from groundwater emissions, we would expect even a negative correlation because the transport of CO₂ from the groundwater surface to the sediment surface should be inhibited by a larger unsaturated zone.
- Higher CO₂ emissions were not accompanied by higher Rn emissions. Groundwater typically contains high Rn concentrations, and Rn is a proven tracer to investigate groundwater input into surface waters (Perkins et al., 2015; Cook and Herczeg, 2000). We observed emission of Rn from the sediments indicating some influence of

groundwater on the sediments. Rn emission at different distances from the river was identical. Thus, the thickness of the unsaturated sediment did not affect Rn emissions, showing that the anoxic zone itself was probably not a source of Rn. Soil Rn concentrations are known to be affected by meteorological and soil physical conditions (Asher-Bolinder et al., 1971). Similar Rn emissions, as observed in our study, are therefore an indication for similar sediment physical conditions. However, the magnitude of Rn emissions did not correspond to the magnitude of the CO₂ emissions, indicating that the CO₂ flux was independent from groundwater outgassing.

- As we did not see hydraulic gradients indicative of larger groundwater inflow at our location of study, CO₂ concentrations in the groundwater were too low to explain the observed CO₂ flux. Groundwater degassing is relevant in situations when groundwater is pumped to the surface (Wood and Hyndman, 2017) or seeps into

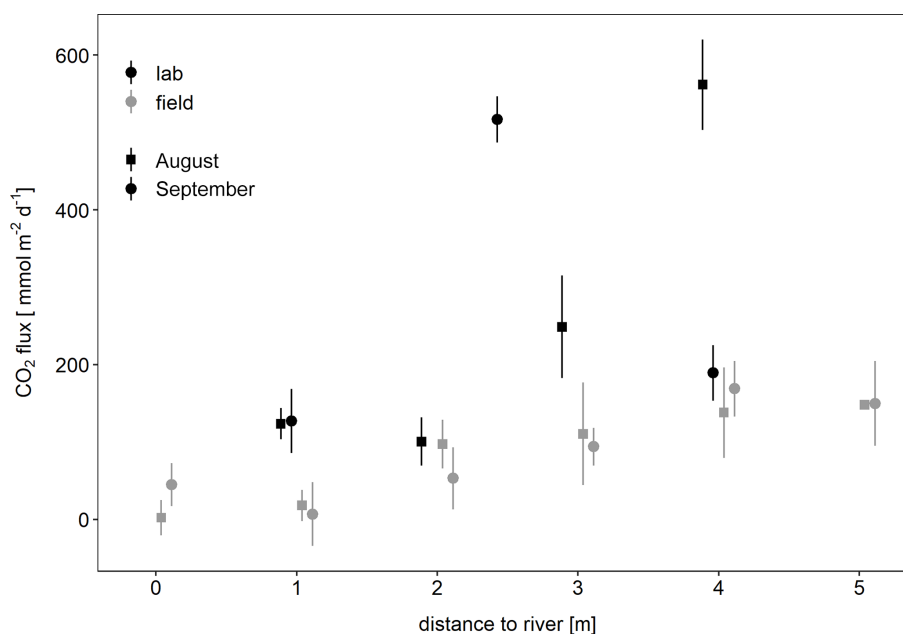


Figure 6. Potential CO₂ flux determined from laboratory incubations of sediment compared to in situ CO₂ fluxes depending on distance to the river. Potential fluxes per unit area were calculated from sediment respiration rates [mmol g-dw⁻¹ d⁻¹], the thickness of the unsaturated zone [cm], and the bulk density of the sediment [g-dw cm⁻³].

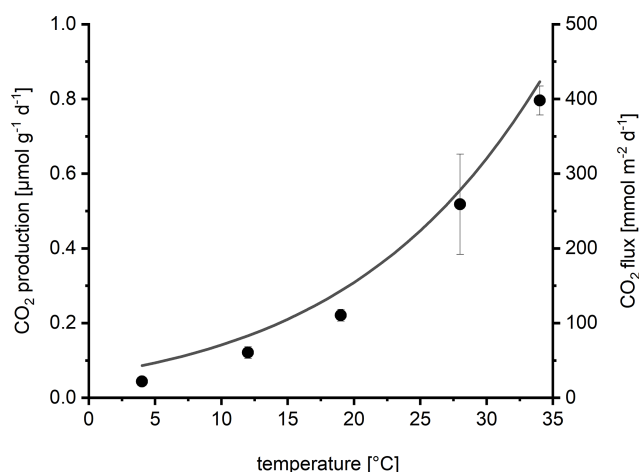


Figure 7. Temperature dependence of sediment CO₂ production (sediment respiration) in laboratory incubations depending on temperature (dots show mean \pm SD of four replicates). For comparison, the line shows the average temperature response of the CO₂ flux measured by automatic chambers, calculated by fitting the data from Fig. 3a to the Arrhenius equation.

surface waters (Duvert et al., 2018). In rivers it might be relevant at seep sites which probably especially occur after fast water level drops and at extremely low water level.

Taken together our data consistently show that the observed CO₂ emissions originated from respiratory CO₂ production

in the sediment. After having identified the primary source of CO₂ we now look on the regulators of the magnitude of the CO₂ emissions.

4.2 Regulation of CO₂ emissions

Temperature is a master variable regulating several biogeochemical processes. Our temperature dependence ($Q_{10} = 2.5$, $E_a = 0.7$ eV) is in line with the temperature response of numerous ecological processes. A meta-analysis of 63 studies of temperature dependence of soil respiration revealed a mean Q_{10} of 2.6 (Hamdi et al., 2013). Diverse types of ecosystems have an activation energy of respiration of 0.65 eV (Yvon-Durocher et al., 2012) which is very similar to our study.

Temperature was an important regulator not only because of the temperature dependence of sediment respiration but also because the diurnal temperature amplitude was quite large. Sediment temperature not only ranged between 2.8 and 32 °C during the study period, but the complete temperature amplitude of about 20 °C could be observed during single days (Fig. 4). The large diurnal amplitude at these sites is favored by a lack of shadow and the fast heating of the sand which can lead to temperatures easily exceeding 40 °C (Mal-last et al., 2020).

Although the temperature dependence of the CO₂ flux is evident, it was not easily visible in flux versus temperature plots which show a large scatter (Fig. 3a). Only when looking at single days, a typical hysteresis pattern (Fig. 3b) became apparent. Such hysteresis curves have frequently been

observed in high-frequency datasets of soil respiration (e.g., Riveros-Iregui et al., 2007). They originate from a phase lag between temperature and CO₂ flux and can be explained by different transport of heat and CO₂ in soils (Phillips et al., 2011) or by variable C supply from plants (Oikawa et al., 2014). The rotation direction as well as the shape of the ellipsoid depends on the vertical profile of temperature and activity in the soils as well as on the depth where soil temperature was measured. We measured temperature in 5 cm depth and obtained counterclockwise hysteresis which means that CO₂ emissions were delayed relative to temperature measurements. A plausible explanation is that a large part of the CO₂ was produced in deeper sediment layers where the daily temperature maximum was reached later. This is consistent with the observed positive correlation between CO₂ flux and the thickness of the unsaturated zone. Theoretically the effect could also be caused by delayed outgassing of CO₂ from deeper sediment layers due to CO₂ transport limitation. However model calculations had shown that this mechanism was less relevant for shaping diurnal hysteresis in soils (Phillips et al., 2011). We quantified the delay by shifting flux and sediment–temperature data against each other (Fig. 8). By correlating the flux with the temperature 3 h before, we obtained the best linear correlation ($R^2 = 0.97$) for the data in Fig. 3b. However, the time shift which produced the best linear fit differed between days (min = 0, max = 10, mean \pm SD = 4.8 ± 3.7 h) with a median of 4 h and no apparent differences between sites. Also the R^2 of the best fit differed between 0.2 and 0.97. Thus, the hysteresis pattern obviously depended on the day of measurement and it is not possible to derive a general relation which then could be used to analyze temperature–flux relations of time-shift-corrected data.

Wetting of dry soils typically triggers a pulse of CO₂ production (Birch, 1958). However, in our case wetting events caused by rainfall reduced the CO₂ flux as exemplified in Fig. 4. This shows that CO₂ production in the sediment was not water limited and/or that the CO₂ flux was rather transport limited when rainwater blocked gas-filled pores (Asher-Bolinder et al., 1971). At sediment moisture around 30 % in sandy sediments as measured in our study microbial activity in the sediment is probably not water stressed and consequently not stimulated by wetting. Thus, it is probable that the reduced CO₂ flux after rain events was caused by physical blocking of soil pores. This is consistent with the observed long-term increase of the CO₂ flux with decreasing moisture. Direct mechanistic dependence, however, is difficult to show because moisture also correlates with the thickness of the unsaturated zone (water level of the river relative to the sediment surface). This is why adding moisture to our mixed model only marginally increased the predictive power of the statistical model.

The thickness of the unsaturated zone was a strong predictor of the CO₂ flux. The entire unsaturated zone obviously contributed to the CO₂ flux. This is plausible because the

intermediate sediment moisture both favored microbial processes and enabled gas exchange through gas-filled pores. This may also explain high CO₂ fluxes in situations with extremely high sediment surface temperature (Mallast et al., 2020). Even if under such conditions CO₂ production is inhibited at the surface, respiration in deeper layers may maintain high CO₂ emissions.

The occurrence of vegetation, although excluded from our chamber measurements and restricted to the vicinity of the chambers, obviously is a game changer, largely stimulating sediment CO₂ emissions. From our data we cannot fully distinguish whether higher fluxes near plants were caused by the plants or only by distance to the water (which is equivalent to the thickness of the unsaturated zone). However, the thickness of the unsaturated zone increased continuously, while the plant line represents a sudden change of conditions. Our data show a consistent high CO₂ flux above the plant line. It is known that root respiration may contribute about 50 % to soil respiration (Hanson et al., 2000) and soil respiration is typically correlated with root biomass (Tufekcioglu et al., 2001). Thus, as we did not use trenched collars to exclude roots from chamber fluxes, it is highly probable that plants contributed to the elevated CO₂ emissions through root respiration or provision of root exudates above the plant line. Higher sediment CO₂ emissions, however, do not mean net CO₂ emissions from the ecosystem since the vegetation growing on the dry sediments also fixes carbon and can even turn exposed sediments into a carbon sink (Bolpagni et al., 2017). To assess the effect of emerging vegetation on the overall carbon cycle of dry sediments, other methods like plant biomass determination or flux measurements including photosynthesis in transparent chambers are necessary.

4.3 CO₂ uptake by the sediment

We frequently observed CO₂ uptake by the sediment, although there were no plants and no light in our chamber. This is known from other studies and has been attributed to inorganic processes (Ma et al., 2013; Marcé et al., 2019). In our case the observed CO₂ uptake could also be explained by the interaction of the sediment with river water. During May and June the river was undersaturated with CO₂ (Fig. S4). The groundwater chemistry data show a gradient of concentrations increasing with distance to the river. This shows that the sediment pore water near to the river was affected by river water. Interestingly, negative fluxes were nearly exclusively observed during the daylight hours. A plausible explanation would be that ship-induced wave action might have triggered occasional river water intrusion and CO₂ uptake by the sediment (Hofmann et al., 2010). This mechanism, however, cannot explain negative fluxes in September when the river was oversaturated with CO₂ (Fig. S4).

Dark CO₂ uptake could theoretically be caused by chemoautotrophic micro-organisms like nitrifiers. However, chemoautotrophic CO₂ uptake should not be stimulated by

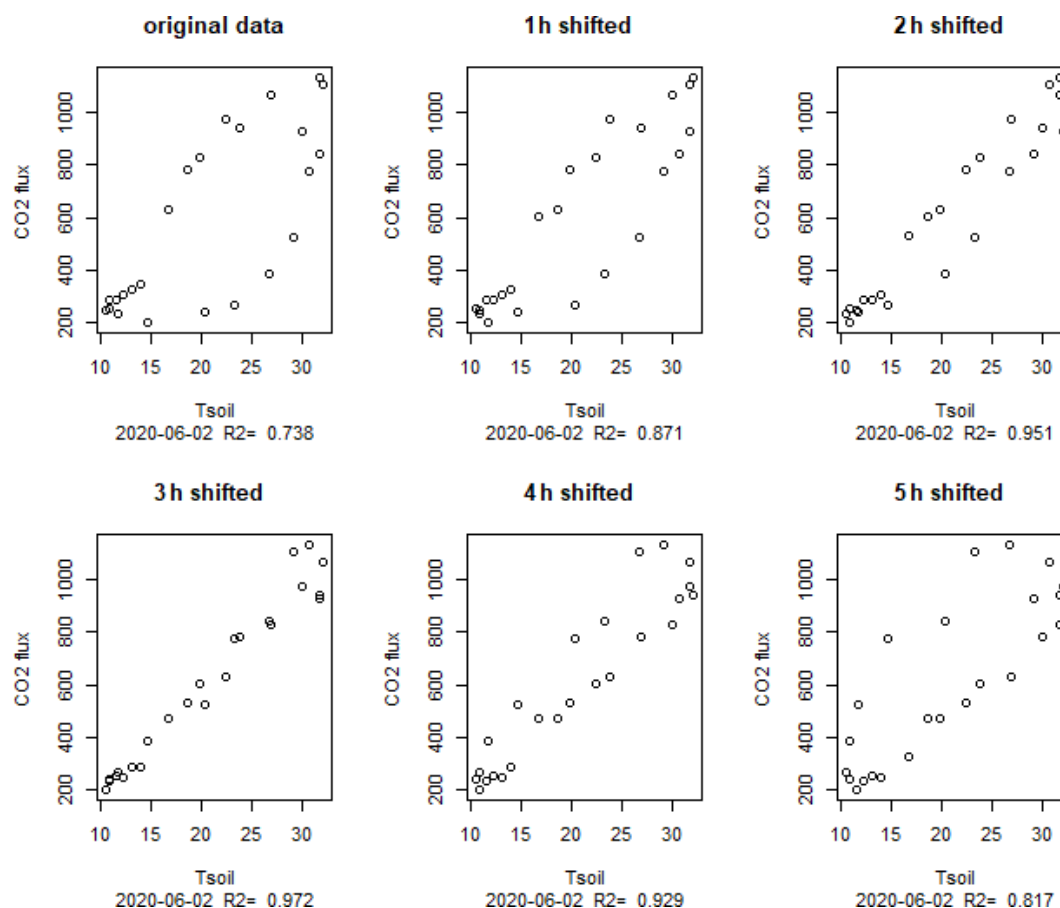


Figure 8. Hysteresis loop for 2 June (same data as in Fig. 3b) with flux data shifted for various hours; 3 h shifted means that the flux at 10:00 local time (CEST) was correlated with the temperature at 07:00.

light and is thus not consistent with our observation of nearly exclusive CO₂ uptake during the day.

A straightforward explanation for negative CO₂ fluxes during the day is CO₂ uptake by phototrophic organisms. Algae and cyanobacteria are known to have active carbon concentrating mechanisms (CCMs) which allow CO₂ uptake also in the dark (Giordano et al., 2005). Phototrophs living at the surface of dry sediments are facing a harsh environment with high salinity in thin water films covering particles and high irradiation and temperature – all factors favoring the activation of CCMs (Beardall and Giordano, 2002). Dark CO₂ uptake is a common observation in ¹⁴CO₂ uptake measurements and known to depend on pre-darkness light conditions (Legendre et al., 1983). In pure cultures, it has been shown that CO₂ uptake by algae may proceed for more than an hour in darkness (Goldman and Dennett, 1986; Ohmori et al., 1984). Thus, it is highly plausible that the observed CO₂ uptake by dry sediments was caused by photosynthetic algae and/or cyanobacteria. Future studies including chlorophyll analysis of sediments or the application of specific inhibitors may clarify the mechanism behind CO₂ uptake in exposed river sediments.

4.4 Implications

Photosynthetic uptake of CO₂ in the dark would have consequences for the interpretation of dark chamber measurements. If a chamber is placed on the sediment, photosynthetic CO₂ uptake may proceed for an unknown period of time. The fact that no net uptake was observed in the night shows that the capability of dark CO₂ uptake could not be sustained for periods longer than 1 h, which is consistent with pure culture observations (Goldman and Dennett, 1986). However, flux measurements are usually performed within a few minutes making it highly probable that they include eventual photosynthetic CO₂ uptake. Comparison of transparent and opaque chamber measurements are sometimes used to detect photosynthesis of algae. Our results imply that such interpretation have to be treated with care because photosynthetic CO₂ uptake may proceed during dark flux measurements.

Our median CO₂ flux of 98 mmol m⁻² d⁻¹ would result in annual emissions of 429 g C m⁻² yr⁻¹ which is in the range of fluxes typical for temperate ecosystems (Doering et al., 2011) and similar to fluxes reported for dry Elbe sediments (Mallast et al., 2020) but high compared to the

gravel bed of an alpine river ($38 \text{ mmol m}^{-2} \text{ d}^{-1}$, Doering et al., 2011), and low compared to exposed sediments of Mediterranean streams ($781 \text{ mmol m}^{-2} \text{ d}^{-1}$, Gómez-Gener et al., 2016). Although our observations thus fit the reported range, these differences as well as the large variation of fluxes observed in our high-frequency measurements (-120 to $1135 \text{ mmol m}^{-2} \text{ d}^{-1}$ – this range is larger than the range of typical fluxes for all kinds of terrestrial ecosystems as compiled by Doering et al., 2011) imply that care must be taken when upscaling fluxes not only for certain ecosystems but also for larger scales.

The observed hysteresis obscures flux–temperature relations if measurements were only performed at one time during the day. Thus, temperature regulation of dry sediment CO₂ emissions might be more relevant and more complex than identified in a recent study (Keller et al., 2020).

Our high-frequency measurements show that standard measuring protocols are probably underestimating CO₂ emissions from dry sediments because high fluxes in the night resulting from a delayed temperature response are not considered. The median flux measured between normal working hours (08:00–18:00) was $87 \text{ mmol m}^{-2} \text{ d}^{-1}$ compared to $98 \text{ mmol m}^{-2} \text{ d}^{-1}$ if all data were considered. Thus, only measuring during daytime would lead to a flux underestimation of 11 %. We therefore recommend to assess temporal shifts in flux–temperature responses in order to obtain better estimates for upscaling based on a representative choice of flux data.

Our results are partly contradicting results from Mallast et al. (2020) who observed highest CO₂ emissions near to the waterline. The two studies, however, are not directly comparable because the previous study by Mallast et al. (2020) was carried out under extreme drought conditions. Under such conditions, deeper lying sediments, which tend to be higher in organic matter and less sandy, were exposed to the atmosphere. Such conditions should favor CO₂ emissions (Keller et al., 2020). Furthermore the very dry conditions ($< 10\%$ sediment moisture) under the extreme drought might have inhibited microbial processes in the sandy sediment. While the drivers of CO₂ emissions from dry sediments are known, their complex interaction makes it difficult to predict CO₂ emissions under a given situation.

The observed relation between CO₂ flux and distance to the river, however, might facilitate upscaling of CO₂ emissions from dry river sediments. The width of the dry sediment zone can be extracted from satellite images or aerial photographs. The observed consistent spatial pattern also implies that the CO₂ flux was probably not much affected by time after exposure. Thus, combining few diurnal datasets of CO₂ flux and lateral transects with seasonal data of the width of the dry sediments zone along a river is a promising approach to quantify total CO₂ emissions from such systems.

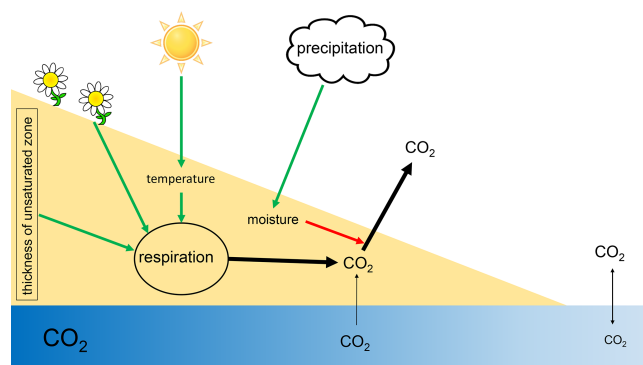


Figure 9. Scheme of processes and drivers of CO₂ fluxes from dry river sediments. Green arrows indicate positive effects; red arrows indicate negative effects.

5 Conclusions

We could clearly show that CO₂ emissions from dry river sediments under the given conditions here were primarily driven by respiration in the sediment. Thus, existing knowledge about soil respiration might also apply to dry river sediments.

We could further show that CO₂ emissions were regulated by temperature and the thickness of the unsaturated zone (Fig. 8). The observed hysteresis effect clearly shows that simple correlations between environmental parameters and CO₂ emissions from sediments may be too simplistic to study regulatory mechanisms. Positively spoken the analysis of such hysteresis relations may allow conclusions about underlying mechanisms (Musolff et al., 2021).

Our data show that the occurrence of terrestrial vegetation has a large and not yet assessed impact on the carbon cycle of dry sediments. To assess the effect of vegetation, not only ecosystem production but also the fate of plant biomass upon re-flooding has to be quantified. While it is clear that CO₂ emissions from dry river sediments are relevant, the exact quantification of the effect of low river levels on the river carbon cycle remains challenging. Short-term temporal variability is very high and probably equally relevant as seasonal variability. Any attempt to quantify annual GHG emissions or the relevance of dry river sediments for carbon cycling needs to address temporal dynamics of CO₂ emissions from dry river sediments.

Data availability. The high-frequency dataset is supplied as a Supplement.

Supplement. The supplement related to this article is available online at: <https://doi.org/10.5194/bg-19-5221-2022-supplement>.

Author contributions. MK initiated the study and prepared the manuscript with contributions from all co-authors. LT and MK performed measurements. All authors planned measurements and discussed the results.

Competing interests. The contact author has declared that none of the authors has any competing interests.

Disclaimer. Publisher's note: Copernicus Publications remains neutral with regard to jurisdictional claims in published maps and institutional affiliations.

Acknowledgements. Thanks to Martin Wieprecht for his excellent help during fieldwork and to Ulrike Berning-Mader and Corinna Völkner for their instructions and help in the laboratory of the University of Münster and UFZ. Thanks to Christian Wilhelm for advice regarding dark CO₂ fixation, Bertram Boehrer for discussion and Peifang Leng for help using R.

Financial support. This work was supported by funding from the Helmholtz Association in the framework of Modular Observation Solutions for Earth Systems (MOSES).

The article processing charges for this open-access publication were covered by the Helmholtz Centre for Environmental Research – UFZ.

Review statement. This paper was edited by Gabriel Singer and reviewed by Kenneth Thorø Martinsen and one anonymous referee.

References

- Asher-Bolinder, S., Owen, D. E., and Schumann, R. R.: A preliminary evaluation of environmental factors influencing day-to-day and seasonal soil-gas radon concentrations, in: *Field Studies of radon in rocks, soils, and water*, edited by: Gundersen, L. C. S. and Wanty, R. B., US Geological Survey, Washington DC, ISBN 9781003070177, 1971.
- Battin, T. J., Luyssaert, S., Kaplan, L. A., Aufdenkampe, A. K., Richter, A., and Tranvik, L. J.: The boundless carbon cycle, *Nat. Geosci.*, 2, 598–600, <https://doi.org/10.1038/ngeo618>, 2009.
- Beardall, J. and Giordano, M.: Ecological implications of microalgal and cyanobacterial CO₂ concentrating mechanisms, and their regulation, *Funct. Plant Biol.*, 29, 335–347, <https://doi.org/10.1071/PP01195>, 2002.
- Birch, H. F.: The effect of soil drying on humus decomposition and nitrogen availability, *Plant Soil*, 10, 9–31, <https://doi.org/10.1007/bf01343734>, 1958.
- Bolpagni, R., Folegot, S., Laini, A., and Bartoli, M.: Role of ephemeral vegetation of emerging river bottoms in modulating CO₂ exchanges across a temperate large lowland river stretch, *Aquat. Sci.*, 79, 149–158, <https://doi.org/10.1007/s00027-016-0486-z>, 2017.
- Bolpagni, R., Laini, A., Mutti, T., Viaroli, P., and Bartoli, M.: Connectivity and habitat typology drive CO₂ and CH₄ fluxes across land–water interfaces in lowland rivers, *Ecohydrology*, 12, e2036, <https://doi.org/10.1002/eco.2036>, 2019.
- Bussmann, I., Koedel, U., Schütze, C., Kamjunke, N., and Koschorreck, M.: Spatial Variability and Hotspots of Methane Concentrations in a Large Temperate River, *Front. Env. Sci.-Switz.*, 10, 833936, <https://doi.org/10.3389/fenvs.2022.833936>, 2022.
- Cook, P. G. and Herczeg, A. L.: *Environmental Tracers in Subsurface Hydrology*, Springer, Boston, 529 pp., ISBN 9780792377078, 2000.
- Coppola, E., Verdecchia, M., Giorgi, F., Colaiuda, V., Tomassetti, B., and Lombardi, A.: Changing hydrological conditions in the Po basin under global warming, *Sci. Total Environ.*, 493, 1183–1196, <https://doi.org/10.1016/j.scitotenv.2014.03.003>, 2014.
- Dell, A. I., Pawar, S., and Savage, V. M.: Systematic variation in the temperature dependence of physiological and ecological traits, *P. Natl. Acad. Sci. USA*, 108, 10591–10596, <https://doi.org/10.1073/pnas.1015178108>, 2011.
- Doering, M., Uehlinger, U., Ackermann, T., Woodtli, M., and Tockner, K.: Spatiotemporal heterogeneity of soil and sediment respiration in a river-floodplain mosaic (Tagliamento, NE Italy), *Freshwater Biol.*, 56, 1297–1311, <https://doi.org/10.1111/j.1365-2427.2011.02569.x>, 2011.
- Duvert, C., Butman, D. E., Marx, A., Ribolzi, O., and Hutley, L. B.: CO₂ evasion along streams driven by groundwater inputs and geomorphic controls, *Nat. Geosci.*, 11, 813–818, <https://doi.org/10.1038/s41561-018-0245-y>, 2018.
- DWD: Datenbasis, Einzelwerte gemittelt, DWD [data set], ftp://opendata.dwd.de/climate_environment/CDC/observations_germany/climate/hourly/, last access: 3 March 2020.
- ELWIS: Wasserstände & Vorhersagen an schiffahrtsrelevanten Pegeln, Pegel Magdeburg-Strombrücke, ELWIS [data set], <https://www.elwis.de/DE/dynamisch/gewaesserkunde/wasserstaende/index.php?target=1&pegelId=cccb57f-a2f9-4183-ae88-5710d3afaefd>, last access: 11 August 2020.
- FAO: Soil testing methods: global soil doctors programme – a farmer to farmer training programme, Soil testing methods manual, FAO (Food and Agriculture Organization of the United Nations), ISBN 9789251311950, 2020.
- Federer, C. A.: BROOK 90: A simulation model for evaporation, soil water, and streamflow, GitHub, https://github.com/rkronen/Brook90_R (last access: 15 November 2022), 2002.
- Gillooly, J. F., Brown, J. H., West, G. B., Savage, V. M., and Charnov, E. L.: Effects of size and temperature on metabolic rate, *Science*, 293, 2248–2251, <https://doi.org/10.1126/science.1061967>, 2001.
- Giordano, M., Beardall, J., and Raven, J. A.: CO₂ concentrating mechanisms in algae: Mechanisms, environmental modulation, and evolution, *Annu. Rev. Plant Biol.*, 56, 99–131, <https://doi.org/10.1146/annurev.arplant.56.032604.144052>, 2005.
- Goldman, J. C. and Dennett, M. R.: Dark CO₂ Uptake by the Diatom Chaetoceros-Simples in Response to Nitrogen Pulsing, *Mar. Biol.*, 90, 493–500, <https://doi.org/10.1007/Bf00409269>, 1986.

- Gómez-Gener, L., Obrador, B., von Schiller, D., Marce, R., Casas-Ruiz, J. P., Proia, L., Acuna, V., Catalan, N., Munoz, I., and Koschorreck, M.: Hot spots for carbon emissions from Mediterranean fluvial networks during summer drought, *Biogeochemistry*, 125, 409–426, <https://doi.org/10.1007/s10533-015-0139-7>, 2015.
- Gómez-Gener, L., Obrador, B., Marcé, R., Acuña, V., Catalán, N., Casas-Ruiz, J. P., Sabater, S., Muñoz, I., and Schiller, D.: When Water Vanishes: Magnitude and Regulation of Carbon Dioxide Emissions from Dry Temporary Streams, *Ecosystems*, 19, 710–723, <https://doi.org/10.1007/s10021-016-9963-4>, 2016.
- Hamdi, S., Moyano, F., Sall, S., Bernoux, M., and Chevallier, T.: Synthesis analysis of the temperature sensitivity of soil respiration from laboratory studies in relation to incubation methods and soil conditions, *Soil Biol. Biochem.*, 58, 115–126, <https://doi.org/10.1016/j.soilbio.2012.11.012>, 2013.
- Hanson, P. J., Edwards, N. T., Garten, C. T., and Andrews, J. A.: Separating root and soil microbial contributions to soil respiration: A review of methods and observations, *Biogeochemistry*, 48, 115–146, <https://doi.org/10.1023/A:1006244819642>, 2000.
- Hofmann, H., Federwisch, L., and Peeters, F.: Wave-induced release of methane: Littoral zones as a source of methane in lakes, *Limnol. Oceanogr.*, 55, 1990–2000, <https://doi.org/10.4319/lo.2010.55.5.1990>, 2010.
- Keller, P. S.: glimr: Compute gasfluxes with R, Gas Fluxes and Dynamic Chamber Measurements, GitHub [code], <https://github.com/tekknosol/glimr> (last access: 15 November 2022), 2020.
- Keller, P. S., Catalán, N., von Schiller, D., Grossart, H. P., Koschorreck, M., Obrador, B., Frassl, M. A., Karakaya, N., Barros, N., Howitt, J. A., Mendoza-Lera, C., Pastor, A., Flaim, G., Aben, R., Riis, T., Arce, M. I., Onandia, G., Paranaíba, J. R., Linkhorst, A., del Campo, R., Amado, A. M., Cauvy-Fraunié, S., Brothers, S., Condon, J., Mendonça, R. F., Reverey, F., Rõõm, E. I., Detry, T., Roland, F., Laas, A., Obertegger, U., Park, J. H., Wang, H., Kosten, S., Gómez, R., Feijoó, C., Eloşegi, A., Sánchez-Montoya, M. M., Finlayson, C. M., Melita, M., Oliveira Junior, E. S., Muniz, C. C., Gómez-Gener, L., Leigh, C., Zhang, Q., and Marcé, R.: Global CO₂ emissions from dry inland waters share common drivers across ecosystems, *Nat. Commun.*, 11, 2126, <https://doi.org/10.1038/s41467-020-15929-y>, 2020.
- Kidron, G. J. and Kronenfeld, R.: Temperature rise severely affects pan and soil evaporation in the Negev Desert, *Ecology*, 9, 1130–1138, <https://doi.org/10.1002/eco.1701>, 2016.
- Koschorreck, M., Prairie, Y. T., Kim, J., and Marcé, R.: Technical note: CO₂ is not like CH₄ – limits of and corrections to the headspace method to analyse pCO₂ in fresh water, *Biogeosciences*, 18, 1619–1627, <https://doi.org/10.5194/bg-18-1619-2021>, 2021.
- Legendre, L., Demers, S., Yentsch, C. M., and Yentsch, C. S.: The C-14 Method – Patterns of Dark CO₂ Fixation and DCMU Correction to Replace the Dark Bottle, *Limnol. Oceanogr.*, 28, 996–1003, <https://doi.org/10.4319/lo.1983.28.5.0996>, 1983.
- Leyer, I. and Wesche, K.: *Multivariate Statistik in der Ökologie. Eine Einführung*, Springer, Berlin, <https://doi.org/10.1007/978-3-540-37706-1>, 2007.
- Ma, J., Wang, Z.-Y., Stevenson, B. A., Zheng, X.-J., and Li, Y.: An inorganic CO₂ diffusion and dissolution process explains negative CO₂ fluxes in saline/alkaline soils, *Sci. Rep.-UK*, 3, 2025, <https://doi.org/10.1038/srep02025>, 2013.
- Machado dos Santos Pinto, R., Weigelhofer, G., Diaz-Pines, E., Guerreiro Brito, A., Zechmeister-Boltenstern, S., and Hein, T.: River-floodplain restoration and hydrological effects on GHG emissions: Biogeochemical dynamics in the parafluvial zone, *Sci. Total Environ.*, 715, 136980, <https://doi.org/10.1016/j.scitotenv.2020.136980>, 2020.
- Macpherson, G. L.: CO₂ distribution in groundwater and the impact of groundwater extraction on the global C cycle, *Chem. Geol.*, 264, 328–336, <https://doi.org/10.1016/j.chemgeo.2009.03.018>, 2009.
- Mallast, U., Staniek, M., and Koschorreck, M.: Spatial upscaling of CO₂ emissions from exposed river sediments of the Elbe River during an extreme drought, *Ecology*, 13, e2216, <https://doi.org/10.1002/eco.2216>, 2020.
- Marcé, R., Obrador, B., Gómez-Gener, L., Catalán, N., Koschorreck, M., Arce, M. I., Singer, G., and von Schiller, D.: Emissions from dry inland waters are a blind spot in the global carbon cycle, *Earth-Sci. Rev.*, 188, 240–248, <https://doi.org/10.1016/j.earscirev.2018.11.012>, 2019.
- Martinsen, K. T., Kragh, T., and Sand-Jensen, K.: Carbon dioxide fluxes of air-exposed sediments and desiccating ponds, *Biogeochemistry*, 144, 165–180, <https://doi.org/10.1007/s10533-019-00579-0>, 2019.
- Matoušů, A., Rulík, M., Tušer, M., Bednářík, A., Šimek, K., and Bussmann, I.: Methane dynamics in a large river: a case study of the Elbe River, *Aquat. Sci.*, 81, 12, <https://doi.org/10.1007/s00027-018-0609-9>, 2019.
- Megonigal, J. P., Brewer, P. E., and Knee, K. L.: Radon as a natural tracer of gas transport through trees, *New Phytol.*, 225, 1470–1475, 2020.
- Musolff, A., Zhan, Q., Dupas, R., Minaudo, C., Fleckenstein, J. H., Rode, M., Dehaspe, J., and Rinke, K.: Spatial and Temporal Variability in Concentration-Discharge Relationships at the Event Scale, *Water Resour. Res.*, 57, e2020WR029442, <https://doi.org/10.1029/2020WR029442>, 2021.
- Ohmori, M., Miyachi, S., Okabe, K., and Miyachi, S.: Effects of Ammonia on Respiration, Adenylate Levels, Amino-Acid Synthesis and CO₂ Fixation in Cells of *Chlorella-Vulgaris* 11h in Darkness, *Plant Cell Physiol.*, 25, 749–756, 1984.
- Oikawa, P. Y., Grantz, D. A., Chatterjee, A., Eberwein, J. E., Allsman, L. A., and Jenerette, G. D.: Unifying soil respiration pulses, inhibition, and temperature hysteresis through dynamics of labile soil carbon and O₂, *J. Geophys. Res.-Biogeo.*, 119, 521–536, <https://doi.org/10.1002/2013JG002434>, 2014.
- Palmia, B., Leonardi, S., Viaroli, P., and Bartoli, M.: Regulation of CO₂ fluxes along gradients of water saturation in irrigation canal sediments, *Aquat. Sci.*, 83, 18, <https://doi.org/10.1007/s00027-020-00773-5>, 2021.
- Penman, H. L.: Natural Evaporation from Open Water, Bare Soil and Grass, *Proc. R. Soc. Lon. Ser.-A*, 193, 120–145, <https://doi.org/10.1098/rspa.1948.0037>, 1948.
- Perkins, A. K., Santos, I. R., Sadat-Noori, M., Gatland, J. R., and Maher, D. T.: Groundwater seepage as a driver of CO₂ evasion in a coastal lake (Lake Ainsworth, NSW, Australia), *Environ. Earth Sci.*, 74, 779–792, <https://doi.org/10.1007/s12665-015-4082-7>, 2015.
- Peters, E., Bier, G., van Lanen, H. A. J., and Torfs, P. J. J. F.: Propagation and spatial distribution of drought

- in a groundwater catchment, *J. Hydrol.*, 321, 257–275, <https://doi.org/10.1016/j.jhydrol.2005.08.004>, 2006.
- Phillips, C. L., Nickerson, N., Risk, D., and Bond, B. J.: Interpreting diel hysteresis between soil respiration and temperature, *Glob. Change Biol.*, 17, 515–527, <https://doi.org/10.1111/j.1365-2486.2010.02250.x>, 2011.
- R-Core-Team: R: A language and environment for statistical computing, R Foundation for Statistical Computing [code], Vienna, Austria, ISBN 3900051070, 2016.
- Reichstein, M., Bednorz, F., Broll, G., and Kätterer, T.: Temperature dependence of carbon mineralisation: conclusions from a long-term incubation of subalpine soil samples, *Soil Biol. Biochem.*, 32, 947–958, [https://doi.org/10.1016/S0038-0717\(00\)00002-X](https://doi.org/10.1016/S0038-0717(00)00002-X), 2000.
- Rey, A.: Mind the gap: non-biological processes contributing to soil CO₂ efflux, *Glob. Change Biol.*, 21, 1752–1761, <https://doi.org/10.1111/gcb.12821>, 2015.
- Riveros-Iregui, D. A., Emanuel, R. E., Muth, D. J., McGlynn, B. L., Epstein, H. E., Welsch, D. L., Pacific, V. J., and Wraith, J. M.: Diurnal hysteresis between soil CO₂ and soil temperature is controlled by soil water content, *Geophys. Res. Lett.*, 34, L17404, <https://doi.org/10.1029/2007gl030938>, 2007.
- Schlesinger, W. H. and Melack, J. M.: Transport of organic carbon in the world's rivers, *Tellus*, 33, 172–187, <https://doi.org/10.3402/tellusa.v33i2.10706>, 1981.
- Scholten, M., Anlauf, A., Büchele, B., Faulhaber, P., Henle, K., Kofalk, S., Leyer, I., Meyerhoff, J., Purps, J., Rast, G., and Scholz, M.: The River Elbe in Germany – present state, conflicting goals, and perspectives of rehabilitation, *Arch. Hydrobiol.*, 155, 579–602, 2005.
- Spinoni, J., Vogt, J. V., Naumann, G., Barbosa, P., and Dosio, A.: Will drought events become more frequent and severe in Europe?, *Int. J. Climatol.*, 38, 1718–1736, <https://doi.org/10.1002/joc.5291>, 2018.
- Steward, A. L., von Schiller, D., Tockner, K., Marshall, J. C., and Bunn, S. E.: When the river runs dry: human and ecological values of dry riverbeds, *Front. Ecol. Environ.*, 10, 202–209, <https://doi.org/10.1890/110136>, 2012.
- Tufekcioglu, A., Raich, J. W., Isenhardt, T. M., and Schultz, R. C.: Soil respiration within riparian buffers and adjacent crop fields, *Plant Soil*, 229, 117–124, <https://doi.org/10.1023/A:1004818422908>, 2001.
- UNESCO/IHA: GHG Measurement Guidelines for Freshwater Reservoirs, UNESCO, 138, ISBN 9780956622808, 2010.
- von Schiller, D., Marcé, R., Obrador, B., Gómez-Gener, L., Casas-Ruiz, J. P., Acuna, V., and Koschorreck, M.: Carbon dioxide emissions from dry watercourses, *Inland Waters*, 4, 377–382, <https://doi.org/10.5268/IW-4.4.746>, 2014.
- Weigold, F. and Baborowski, M.: Consequences of delayed mixing for quality assessment of river water: Example Mulde–Saale–Elbe, *J. Hydrol.*, 369, 296–304, <https://doi.org/10.1016/j.jhydrol.2009.02.039>, 2009.
- Weise, L., Ulrich, A., Moreano, M., Gessler, A., E. Kayler, Z., Steger, K., Zeller, B., Rudolph, K., Knezevic-Jaric, J., and Premke, K.: Water level changes affect carbon turnover and microbial community composition in lake sediments, *FEMS Microbiol. Ecol.*, 92, fiw035, <https://doi.org/10.1093/femsec/fiw035>, 2016.
- Wood, W. W. and Hyndman, D. W.: Groundwater Depletion: A Significant Unreported Source of Atmospheric Carbon Dioxide, *Earth's Future*, 5, 1133–1135, <https://doi.org/10.1002/2017ef000586>, 2017.
- Yvon-Durocher, G., Caffrey, J. M., Cescatti, A., Dossena, M., del Giorgio, P., Gasol, J. M., Montoya, J. M., Pumpanen, J., Staehr, P. A., Trimmer, M., Woodward, G., and Allen, A. P.: Reconciling the temperature dependence of respiration across timescales and ecosystem types, *Nature*, 487, 472–476, <https://doi.org/10.1038/Nature11205>, 2012.